Submitted August 31, 2012.

Published on-line on October3, 2012, in

Vacuum 89 (2013) 53-56

http://dx.doi.org/10.1016/j.vacuum.2012.09.002

Estimating electron drift velocities in magnetron discharges

Albert Rauch and André Anders*

Lawrence Berkeley National Laboratory, Plasma Applications Group, Berkeley, CA

*Corresponding Author.
Dr. Andre Anders
Lawrence Berkeley National Laboratory
1 Cyclotron Road, MS 53
Berkeley, CA 94720, USA
Tel. +1-510-486-6745
Fax +1-510-486-4374
aanders@lbl.gov

ACKNOWLEDGEMENTS

The authors thank Matjaz Panjan and Christian Hornschuch for critical discussions. A.R. thanks the Austrian Marshall Plan Foundation for funding a scholarship. A.A. acknowledges support by the Assistant Secretary for Energy Efficiency and Renewable Energy, Office of Building Technology, of the U.S. Department of Energy, under Contract No. DE-AC02-05CH11231.

Estimating electron drift velocities in magnetron discharges

Albert Rauch and André Anders

Lawrence Berkeley National Laboratory, Berkeley, California, USA

Abstract

Electron motion in magnetron discharges is complicated. In a first approximation, single particle motion can be considered in given electric and magnetic fields to estimate drifts. Based on magnetic and electric field measurements for discharges in an unbalanced magnetron with a strong magnet it is shown that, for the most energetic electrons, the ∇B and curvature drift velocities can be comparable to or even larger than the commonly mentioned $\mathbf{E}\times\mathbf{B}$ drift velocity. In the fluid approximation, the electron pressure gradient adds yet another drift component. Since all of those drifts are generally additive, the term "$\mathbf{E}\times\mathbf{B}$ drift" can be generically used but should be understood to include other drifts. Strong velocity gradients and direction reversal can be found, which suggest velocity shear as a source of waves and instabilities, likely creating the density-fluctuation "seeds" for ionization zones seen in high power impulse magnetron sputtering.

Keywords: Magnetron, sputtering, electron drift velocity

1. Introduction: Magnetron operation

Magnetron discharges are widely used in physical vapor deposition. Although a great variety exists in terms of target (cathode) shapes and sizes, they all have in common that energetic electrons are confined near the target by a clever combination of electric and magnetic fields such that energetic electrons execute a closed drift. In this way the magnetron discharge, a magnetically enhanced glow discharge, is enabled to operate at much lower pressure than the common glow discharge, i.e. a glow discharge in the absence of a magnetic field. Much has been published about the magnetron's operational principles and properties [1-12] and therefore it is sufficient to focus here on some relevant details related to the closed electron drifts.

Between collisions, neglecting collective effects, an electron trajectory is determined by the equation of motion

$$m_e\, d\mathbf{v}/dt = -e\left(\mathbf{E}+\mathbf{v}\times\mathbf{B}\right) \tag{1}$$

where m_e is the electron mass, $\mathbf{v}$ is the velocity vector, e is the elementary charge, and $\mathbf{E}$ and $\mathbf{B}$ are the vectors of the local electric field and magnetic field, respectively. The $\mathbf{v}\times\mathbf{B}$ or Lorentz force term makes electrons gyrate around field lines, and the electric field term causes periodic

acceleration and deceleration as the electron gyrate. In the case when the electric and magnetic fields do not strongly vary one can take the local **E** and **B** values and arrives at the well-known $\mathbf{E}\times\mathbf{B}$ drift velocity [13, 14]

$$\mathbf{v}_{ExB} = \mathbf{E}\times\mathbf{B}/B^2 \ . \tag{2}$$

The magnetic field of a magnetron is designed in such a way that the drift of electrons is closed. The less-energetic electrons, however, are subject to many collisions with other electrons and ions and therefore may not arrive at the same location but are much displaced. Cross-**B**-field diffusion and a host of plasma instabilities facilitate the escape of electrons from the target zone to the anode. After all, electrons need to carry the discharge current to the anode.

The actual path of electrons in a magnetron is complicated since the electron motion occurs in non-parallel and non-uniform electric and magnetic fields. Powerful three-dimensional codes need to be employed to realistically describe the processes of electron motion in plasmas, including drifts and transport across the magnetic fields [15].

In this contribution, much simplified considerations are made. We will estimate the $\mathbf{E}\times\mathbf{B}$ drift velocity based on measured **E** and **B** fields, and compare it with other drifts associated with the non-uniformity of the fields. We then also include the electron pressure gradient drift based on plasma parameter estimates.

2. ExB, gradient B, and other drifts

To conceptually understand the drift of electrons in the single particle approximation, one commonly introduces two averaging steps. First, one averages over the gyration motion of the electron to arrive at the motion of the gyration center. If we neglect for a moment the presence of an electric field, the gyration center would follow the magnetic field line, which is generally arched over the target and intersects the target surface (Fig. 1). As the gyration center approaches the target, the velocity component parallel to the magnetic field line reduces since the magnetic field strength increases (see magnetic mirror effect [13, 14]). Now, putting the electric field back in the picture, the electron, before arriving at the target surface, encounters the electric field of the presheath and sheath (the space charge layer adjacent to the target). The electric field component parallel to the magnetic field component sends the gyration center back and forth along the arched magnetic field line. Averaging over this back-and-forth motion reveals a net velocity component which is perpendicular to both the electric and magnetic field. Using characteristic field values one get an estimate for the $\mathbf{E}\times\mathbf{B}$ drift velocity, as described by equation (2).

This description, however, is not complete since the electric and magnetic fields are not uniform: additional drift components appear. Most notably we deal with a magnetic field that strongly loses strength with increasing distance from the target. A gradient in the magnetic field leads to the $\mathbf{B}\times\nabla B$ and higher order drifts [13]. For electrons (taking the sign of the negative charge of electrons into account), the ∇B drift velocity is [13]

$$v_{\nabla B} = \frac{v_\perp r_L}{2} \frac{\nabla B \times \mathbf{B}}{B^2} \tag{3}$$

where

$$r_L = \frac{v_\perp}{\omega_c} = \frac{m_e}{e} \frac{v_\perp}{B} \tag{4}$$

is the gyration or Larmor radius; ω_c is the gyration or cyclotron frequency, and $v_\perp$ is the velocity of the electron motion perpendicular to the **B**-field. Fig. 2 shows the distribution of Larmor radii assuming the gyrating electrons have $v_\perp$ corresponding to an energy of 10 eV. Electrons of higher energy have a correspondingly greater gyration radius. Here lies one of the difficulties: electrons have different velocities perpendicular to the magnetic field, and the values vary accordingly.

Since we are mostly interested in energetic electrons capable of causing ionizing collisions, we may focus on secondary electrons released from the target by primary ion impact or photo-emission. Such electrons gain energy up to the full potential difference dropping in the sheath, ΔV_{se}, when traversing the sheath. The perpendicular velocity is up to a maximum

$$v_{\perp,\max} = \left(\frac{2e\,\Delta V_{se}}{m_e} \right)^{1/2} . \tag{5}$$

and we arrive at the following expression for the maximum ∇B drift velocity:

$$v_{\nabla B,\max} = \frac{v_{\perp,\max}\, r_L}{2} \frac{\nabla B \times \mathbf{B}}{B^2} = \Delta V_{se} \frac{\nabla B \times \mathbf{B}}{B^3} \tag{6}$$

Since ∇B and $\mathbf{E}$ point in the same direction in the most relevant region over the racetrack, the ∇B drift is generally additive to the $\mathbf{E} \times \mathbf{B}$ drift.

We also consider an expression for the curvature drift [13]

$$v_R = -\frac{m_e}{e} v_\parallel^2 \frac{\mathbf{R_c} \times \mathbf{B}}{R_c^2 B^2} \tag{7}$$

where $\mathbf{R_c}$ is the radius vector of the curved magnetic field, and $v_\parallel$ is the velocity component parallel to the magnetic field vector.

Going beyond the single particle description by including a fluid model for electrons, electron drift is also caused by the local gradient of electron pressure. In standard text books like [13], the fluid approximation is introduced for electrons and ions, and the resulting gradient drift is called diamagnetic drift. In our case, we do not consider ions because they are not magnetized due to their high mass. They are therefore not subject to such drift, and we prefer the term electron pressure gradient drift. Taking the negative charge of electrons into account, the electron pressure gradient drift velocity is [13]

$$v_{\nabla p} = \frac{\nabla p_e \times \mathbf{B}}{e n_e B^2} \tag{8}$$

We can write $\nabla p_e = k\left(T_e \nabla n_e + n_e \nabla T_e\right) \approx k T_e \nabla n_e$ because the density can change by orders of magnitude while the electron temperature varies relatively little. By introducing a characteristic length of density change, $d_{\nabla n} = n_e / \nabla n_e$, the absolute value of the gradient drift velocity reduces to

$$\left| v_{\nabla p} \right| = \frac{k T_e}{e B\, d_{\nabla n}} \tag{9}$$

When evaluating those expressions we notice immediately that the magnetic field strength appears in the denominator, which, for non-zero electric field, will make the drift velocities unphysically large where the magnetic field is very small. Clearly, the assumption of magnetization ($r_L \ll$ characteristic system length) can be violated. Therefore, we will not use the expression at small magnetic fields, especially around the magnetic null point.

3. Determining electron drifts for a specific magnetron

We illustrate the situation for a specific magnetron used in our laboratory for recent high power impulse magnetron sputtering (HiPIMS) measurements [16, 17]). This is a 76 mm diameter (3 inch) unbalanced magnetron made by US Inc. (now MeiVac Inc.). Fig. 1 shows the magnetic field strength as measured with a movable Hall probe. Detailed information on the magnetic field distribution helps us to evaluate expressions containing **B** and ∇B and to create maps of Larmor radii and drift velocities. An estimate using Ampere's law indicates that changes of the magnetic field by the magnetron discharge and Hall currents can be neglected unless one works with HiPIMS at high currents. No changes of the magnetic field are considered here.

For the evaluation of the $\mathbf{E} \times \mathbf{B}$ drift we need the electric field, which can be derived from measurements of the plasma potential, $\mathbf{E} = -\nabla V_p$. Such information is difficult to get but we can refer to measurements with emissive probes which have been made at the same magnetron [17]. Unfortunately, the potential measurements excluded the interesting region right over the racetrack since the probe excessively disturbed the discharge when brought too close to the racetrack region. For our magnetron we found $E \sim 10^4$ V/m in the magnetic presheath region [17] and $B \sim 0.06$ T. This results in $v_{ExB} \sim 1-2\times10^5$ m/s with the exception of the region close to the racetrack. Figure 3 shows the spatial velocity distribution excluding regions over the racetrack (lack of electric field data) and near the magnetic null (lack of electron magnetization). The latter region was expected to be exactly on axis, but it appears to be about 3 mm off axis, perhaps due to a misalignment or asymmetry of the permanent magnets and/or positioning errors of the probe relative to the magnetron. More importantly, Fig. 3 indicates strong velocity gradients, especially in the region near the magnetic zero ($z \approx 40$ mm). Velocity gradients indicate shear, which is known to cause instabilities and turbulence, observable as noise in

electrical and particle transport parameters. Density fluctuations may start and amplify due to a positive feedback observed in high power impulse magnetron sputtering, i.e. the velocity gradients generate the conditions for forming the "seeds" of localized ionization zones [18].

For the ∇B drift, we can make a corresponding estimate using the values $\nabla B \approx 60\ \text{mT} / 10\ \text{mm} = 6\ \text{T/m}$ over the racetrack, and $B \approx 0.06\ \text{T}$ in the same region, hence $\nabla B / B^2 \approx 1700\ \text{T}^{-1}\text{m}^{-1}$. For the range of electron energies $e\,\Delta V_{se} \approx 100 - 500\ \text{eV}$ we obtain $v_{\nabla B} \approx 1.6\text{-}8.3 \times 10^5\ \text{m/s}$. The maximum drift velocity field is plotted in Fig. 4 considering the most energetic electrons, assuming 500 eV in energy. We see that in this case, the ∇B drift velocity may be comparable to or even greater than the $\mathbf{E} \times \mathbf{B}$ drift velocity. Looking further from the target we see the above-mentioned issue around the magnetic null, and a reversal of the drift velocity direction with increasing distance from the target. Also here, the reversal of the velocity direction within a relatively tight spatial region suggests that waves, instabilities, and turbulence are generated in this shear zone.

Next, to evaluate the curvature drift, we arbitrarily use values for $v_{\parallel}$ from kT_{e} of a few eV to about ½ of the maximum voltage drop, $v_{\parallel} \leq \left(e\,\Delta V_{se} / m_e\right)^{1/2}$, take $R_c \approx 5\ \text{mm}$, and use $B \approx 0.06\ \text{T}$ to be consistent with the above estimate for the gradient drift for our magnetron example. This results in a wide range of possible velocity values, $v_R \approx 10^4 - 10^6\ \text{m/s}$, which again may reach or exceed the $\mathbf{E} \times \mathbf{B}$ drift velocity.

Finally, we consider the electron pressure gradient drift. Using the same values as before for magnetic field and temperature, and consider $d_{\nabla n} \sim (1-5) \times 10^{-3}\ \text{m}$ (from imaging), we arrive at $\left|v_D\right| \approx (1-5) \times 10^4\ \text{m/s}$. The pressure gradient drift velocity appears to be smaller than the $\mathbf{E} \times \mathbf{B}$ drift velocity but not by much. Also here, since ∇p_e is in the same direction as $\mathbf{E}$, those velocities are additive. We note that Lundin and coworkers [19] came to similar values and conclusions.

4. Summary

Summarizing, simplified estimates using *measured* data of magnetic and electric fields for a specific unbalanced magnetron show that the ∇B drift and the curvature drift may reach values comparable to, or even greater than the usually quoted $\mathbf{E} \times \mathbf{B}$ drift velocities if the electrons are very energetic. Since the drift velocity are approximately pointing in the same direction they are additive. This also applies to the electron pressure gradient drift, which is considered when using the fluid approximation. No gross error is made when generally referring to the $\mathbf{E} \times \mathbf{B}$ drift as long it is understood that other drifts also play a role, especially for the most energetic electrons. This conclusion was derived from data of a specific magnetron where the magnetic field is rather strong and the magnetic null is close to the target. Other magnetrons may not necessarily have such strong ∇B and curvature drift components. Strong velocity gradients, shear, and even direction reversal can be found, which suggests that drifting electrons create waves and instabilities. This is consistent with the understanding that $\mathbf{E} \times \mathbf{B}$ discharges

generally exhibit instabilities, and that seeding for self-organized traveling ionization zones in HiPIMS is readily available.

Acknowledgments

We thank Matjaz Panjan and Christian Hornschuch for critical discussions. A.R. thanks the Austrian Marshall Plan Foundation for funding a scholarship. A.A. acknowledges support by the Assistant Secretary for Energy Efficiency and Renewable Energy, Office of Building Technology, of the U.S. Department of Energy, under Contract No. DE-AC02-05CH11231.

References

[1] J.W. Bradley, G. Lister, Plasma Sources Sci. Technol. 6 (1997) 524.
[2] J.W. Bradley, S. Thompson, Y.A. Gonzalvo, Plasma Sources Sci. Technol. 10 (2001) 490.
[3] G. Bräuer, B. Szyszka, M. Vergöhl, R. Bandorf, Vacuum 84 (2010) 1354.
[4] J.S. Chapin, Vacuum Technology (1974) 37.
[5] D. Depla, S. Mahieu, R. De Gryse, Thin Solid Films 517 (2009) 2825.
[6] S. Kadlec, Surf. Coat. Technol. 202 (2007) 895.
[7] W.D. Münz, Surf. Coat. Technol. 48 (1991) 81.
[8] J. Musil, Surf. Coat. Technol. 100-101 (1998) 280.
[9] S.M. Rossnagel, H.R. Kaufman, J. Vac. Sci. Technol. A 6 (1988) 223.
[10] T.E. Sheridan, M.J. Goeckner, J. Goree, J. Vac. Sci. Technol. A 8 (1990) 1623.
[11] J.A. Thornton, J. Vac. Sci. Technol. 15 (1978) 171.
[12] B. Window, N. Savvides, J. Vacuum Sci. Technol. A 4 (1986) 453.
[13] F.F. Chen, Plasma Physics and Controlled Fusion, Plenum Press, New York, 1984.
[14] J.A. Bittencourt, Fundamentals of Plasma Physics, Springer, New York, 2004.
[15] A. Bogaerts, E. Bultinck, I. Kolev, L. Schwaederlé, K.V. Aeken, G. Buyle, D. Depla, J. Phys D: Appl. Phys. 42 (2009) 194018.
[16] A. Anders, P. Ni, A. Rauch, J. Appl. Phys. 111 (2012) 053304.
[17] A. Rauch, R. Mendelsberg, J.M. Sanders, A. Anders, J. Appl. Phys. 111 (2012) 083302.
[18] A. Anders, Appl. Phys. Lett. 100 (2012) 224104.
[19] D. Lundin, U. Helmersson, S. Kirkpatrick, S. Rohde, N. Brenning, Plasma Sources Sci. Technol. 17 (2008) 025007.

Figure Captions

Fig. 1. Measured magnetic field of a 76 mm (3") magnetron with a 6.2 mm (1/4") thick Nb target in place. As evident by the magnetic null point close to the target, this is an unbalanced magnetron (manufacturer US Inc., now MeiVac Inc.)

Fig. 2. Electron Larmor radius for the measured magnetic field, arbitrarily assuming a constant velocity perpendicular to the magnetic field vector corresponding to 10 eV. The region around the magnetic null is excluded since electrons are not magnetized when the magnetic field is very weak.

Fig. 3 $\mathbf{E}\times\mathbf{B}$ drift velocity field derived from the measured magnetic field and the measured plasma potential field [17]. In the experiment, the voltage on-time was set to 100 μs with a pulse repetition rate of 100 Hz, applied discharge voltage -488 V at an argon pressure 0.26 Pa. The velocity field near the racetrack could not be measured since the disturbance of the discharge plasma by the probe was large. The region near the magnetic zero is excluded due to the lack of electron magnetization.

Fig. 4 Maximum ∇B drift velocity, considering the most energetic electrons by assuming they have gained 500 eV in energy when traversing the sheath. The "hole" in the center is associated with the magnetic null, where electrons lose magnetization.

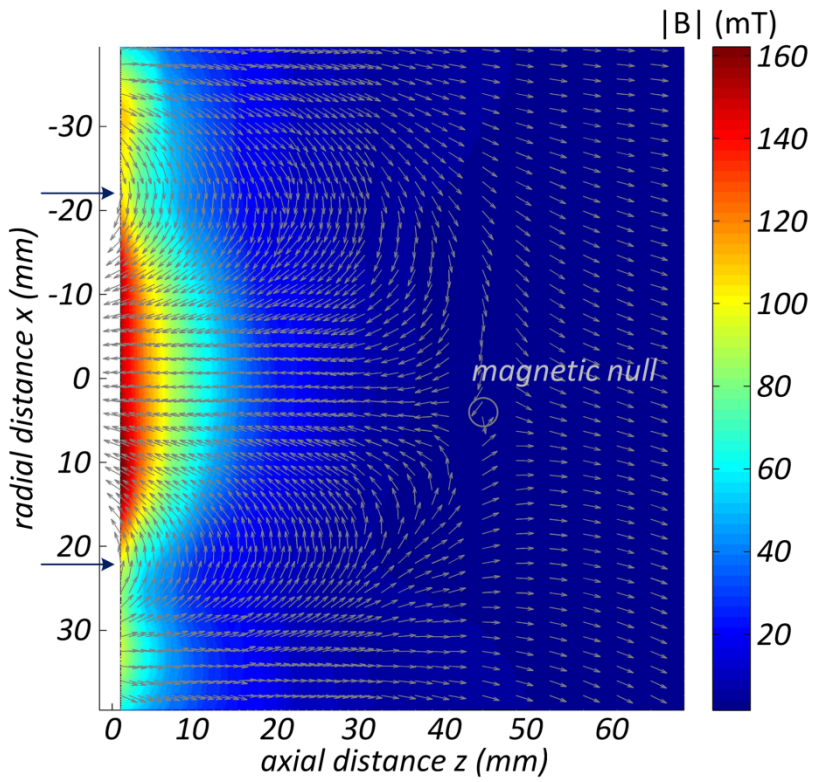
|B| (mT)
160
140
120
100
80
60
40
20
-30
-20
-10
0
10
20
30
radial distance x (mm)
magnetic null
0
10
20
30
40
50
60
axial distance z (mm)

Fig. 1

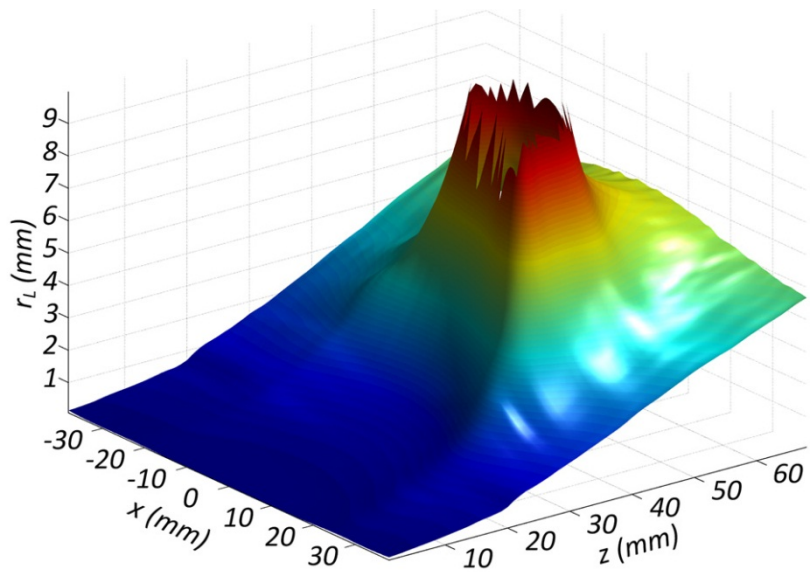

Fig. 2

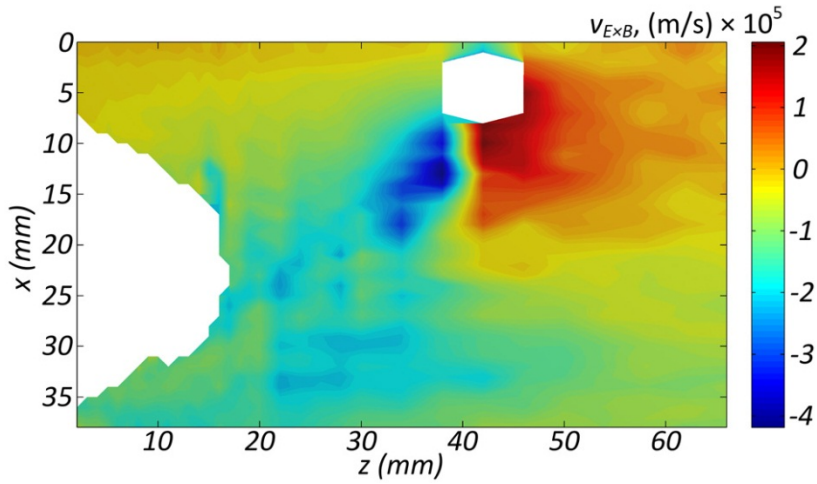
$v_{E\times B}$, (m/s) × 10^5
2
1
0
-1
-2
-3
-4
0
5
10
15
20
25
30
35
x (mm)
10
20
30
40
50
60
z (mm)

Fig. 3

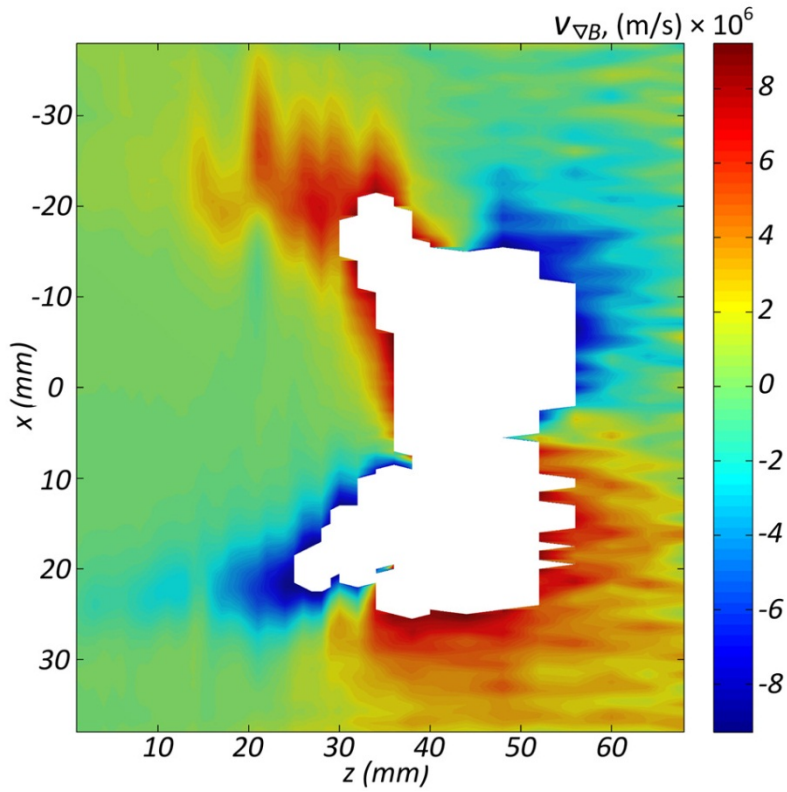
$v_{\nabla B}$, (m/s) × 10^6
8
6
4
2
0
-2
-4
-6
-8
-30
-20
-10
0
10
20
30
x (mm)
10
20
30
40
50
60
z (mm)

Fig. 4